DOI 10.1007/s10812-017-0561-9

Journal of Applied Spectroscopy, Vol. 84, No. 5, November, 2017 (Russian Original Vol. 84, No. 5, September–October, 2017)

SYNTHESIS, VIBRATIONAL SPECTRA, AND DFT SIMULATIONS OF 3-BROMO-2-METHYL-5-(4-NITROPHENYL)THIOPHENE

A. A. Balakit,[a*] Y. Sert,[b,c*] Ç. Çırak,[d] K. Smith,[e] B. M. Kariuki,[e] and G. A. El-Hiti[f*]

UDC 535.375.5;543.42

*A new thiophene derivative, 3-bromo-2-methyl-5-(4-nitrophenyl)thiophene (**2**), was synthesized through the Suzuki coupling reaction of 4-bromo-5-methylthiophen-2-ylboronic acid (**1**) and 4-iodonitrobenzene, and its structure was confirmed by nuclear magnetic resonance (NMR), low and high resolution mass spectrometry (HRMS), Fourier transform infrared spectroscopy (FT-IR), and X-ray investigations of the crystal structure. The FT-IR spectra (4000–400 cm^{-1}), Raman spectra (4000–100 cm^{-1}), and theoretical vibrational frequencies of this new substance were investigated. Its theoretically established geometric parameters and calculated vibrational frequencies are in good agreement with the reported experimental data. The highest occupied molecular orbital (HOMO) and lowest unoccupied molecular orbital (LUMO) energies and other related parameters of the compound were calculated. The ionization potentials given by the B3LYP and HF (Hartree–Fock) methods for this new compound are –0.30456 and –0.30501 eV, respectively.*

Keywords: *FT-IR spectra, Raman spectra, 3-bromo-2-methyl-5-(4-nitrophenyl)thiophene, vibrational frequencies, frontier molecular orbital.*

Introduction. Thiophene derivatives are important compounds that can be used as precursors for the synthesis of materials. They are of great interest due to numerous applications in photoswitching [1, 2], nanotechnologies [3, 4], and biosensorics [5]. Aryl thiophenes are usually synthesized *via* metal catalyzed cross-coupling processes, such as the Suzuki, Negishi, and Stille reactions, in which the organometallic derivatives of thiophene undergo coupling reactions with aryl halides [6, 7]. Also, aryl thiophenes can be synthesized by palladium-catalyzed direct arylation of substituted thiophenes with aryl bromides [8]. 3-Bromo-2-methyl-5-phenylthiophene is one of the most frequently used derivatives. It is usually synthesized via the Suzuki coupling reaction [9, 10].

For our studies of the synthesis and optical properties of various heterocycles [11–16], we synthesized 3-bromo-2-methyl-5-(4-nitrophenyl)thiophene (**2**) and for the first time established its molecular and crystal structures using the methods of Fourier transform infrared spectroscopy (FT-IR), Raman spectroscopy, and quantum chemical calculations for determining the vibrational frequencies.

Experimental. *Characterization techniques.* A Gallenkamp melting point apparatus was used to determine the melting point. ^{1}H (400 MHz) and ^{13}C NMR (100 MHz) spectra were recorded in $CDCl_3$ on a Bruker AV400 spectrometer. Chemical shifts δ (ppm) are reported relative to TMS, and coupling constants (*J*) are in Hz. A Waters GCT Premier Spectrometer was used to record the mass spectrum. A Waters LCT Premier XE setup was used to record the accurate mass of the molecular ion peak. A Perkin-Elmer Spectrum Two FT-IR Spectrometer was used to record the IR spectrum (4000–400 cm^{-1}). A Renishaw Invia Raman spectrophotometer was used to record the Raman spectrum (4000–100 cm^{-1}). X-ray crystallographic data were collected at 150 K on a Nonius Kappa CCD diffractometer using graphite monochromated MoK_α radiation

*To whom correspondence should be addressed.

[a]College of Pharmacy, University of Babylon, P.O. Box 4, Babylon, Iraq; email: asim_alsalehi@hotmail.com; [b]Bozok University, Department of Physics, Faculty of Art & Sciences, Yozgat 66100, Turkey; [c]Sorgun Vocational School, Bozok University, Yozgat 66100, Turkey; email: yusufsert1984@gmail.com; [d]Erzincan University, Department of Physics, Faculty of Art & Sciences, Erzincan 24100, Turkey; [e]School of Chemistry, Cardiff University, Main Building, Park Place, Cardiff CF10 3AT, UK; [f]Cornea Research Chair, Department of Optometry, College of Applied Medical Sciences, King Saud University, P.O. Box 10219, Riyadh 11433, Saudi Arabia; email: gelhiti@ksu.edu.sa. Abstract of article is published in Zhurnal Prikladnoi Spektroskopii, Vol. 84, No. 5, p. 834, September–October, 2017.

($\lambda_{MoK\alpha}$ = 0.71073 Å) equipped with an Oxford Cryosystem of cooling. The structures were solved using direct methods and refined with SHELX [17]. It is established that the structure is a two-component inversion twin. There are two molecules in the asymmetric unit, and the thiophene group is disordered in both with occupancies of 0.129(4)/0.871(4) and 0.342(4)/0.658(4). The molecule geometry was reconstructed with the help of the data provided by The Cambridge Crystallographic Data Centre (www.ccdc.cam.ac.uk/structures).

*Synthesis of 3-bromo-2-methyl-5-(4-nitrophenyl)thiophene (**2**)* (Scheme 1). A mixture of 3-bromo-2-methylthiophen-5-ylboronic acid (**1**) (1.00 g, 4.53 mmol), 4-iodonitrobenzene (1.00 g, 4.02 mmol), anhydrous sodium carbonate (1.28 g, 12.10 mmol), and tetrakis(triphenylphosphine)palladium(0) (0.12 g, 0.11 mmol) in tetrahydrofuran (30 mL, containing 10% water) was refluxed at 90°C for 16 h. The mixture was left to cool to room temperature, after which it was extracted with diethyl ether (3–50 mL). The organic layer was separated, dried ($MgSO_4$), and evaporated under reduced pressure. The obtained crude product was purified by column chromatography (silica gel; petroleum ether 40–60°C/ethyl acetate 97:3 by volume) to give compound **2** (1.00 g, 3.35 mmol; 83%). Crystallization from diethyl ether gave yellow crystals m.p. 131–132°C. ^{1}H NMR, δ: 8.15 (d, *J* = 8.8, 2H, H-3/H-5 of Ar), 7.56 (d, *J* = 8.8, 2H, H-2/H-6 of Ar), 7.2 (s, 1H, H-4), and 2.38 (s, 3H, CH_3). ^{13}C NMR, δ: 146.7 (s, C-4 of Ar), 139.5 (s, C-1 of Ar), 138.2 (s, C-5), 137.0 (s, C-2), 128.2 (d, C-4), 125.4 (d, C-2/C-6 of Ar), 124.5 (d, C-3/C-5 of Ar), 111.0 (s, C-3) and 15.1 (q, CH_3). EI-MS (*m*/*z*, %): 299 ($[M^{81}Br]^+$, 92), 297 ($[M^{79}Br]^+$, 94), 269 (100), 267 (93), 188 (20), 171 (70). HRMS (EI): Found, 296.9452. Calculated for $C_{11}H_8NO_2SBr$ $[M^{79}Br]^+$ 296.9459.

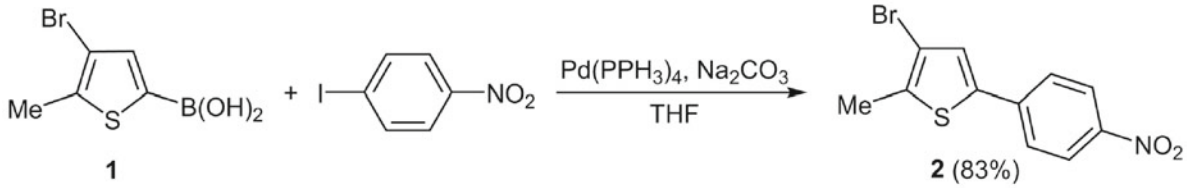

Scheme 1. Synthesis of 3-bromo-2-methyl-5-(4-nitrophenyl)thiophene (**2**).

Computational Details. Initial atomic coordinates were determined using the Gauss View software database and experimental XRD data to optimize the input structure to obtain the most stable structure [18]. The DFT/B3LYP and HF methods with the 6-311++G(d,p) basis set were used to calculate the molecular structures (gas phase ground state) of compound **2**. The vibrational frequencies were then found for the calculated optimized structure. The calculated harmonic vibrational frequencies were scaled by 0.9614 (B3LYP) and 0.9051 (HF) for the use with the 6-311++G(d,p) basis set, respectively [18, 19]. The molecular properties, such as optimized geometric parameters and vibrational wave numbers, were calculated using Gauss View molecular visualization [18] and Gaussian 09W [20] sofware. The calculated vibrational frequencies were assigned via potential energy distribution (PED) analysis of all the fundamental vibration modes by using VEDA 4 software [21, 22]. All the vibrational assignments were based on the B3LYP/6-311++G(d,p) level calculations. Therefore, some assignments might correspond to the value of the previous or next vibrational frequency at the HF/6-311++G(d,p) level.

Results and Discussion. *Geometric structure.* The X-ray analysis of the crystal structure of compound ($C_{11}H_8BrNO_2S$) (**2**) showed an orthorhombic system with the $Pca2_1$ space group. It showed the following cell dimensions: *a* = 26.1513 Å, *b* = 3.8859 Å, *c* = 21.3942 Å, α = 90°, β = 90°, γ = 90°, and *V* = 2174.11 Å^3. Since there are two molecules in the asymmetric unit and the thiophene group is disordered in both, the crystal contains four distinct sets of bond lengths and angles, although they are all very similar. Consequently, just one representative set was used in order to compare the experimental and computational values. The bond lengths and bond angles for the selected experimental (X-ray) and optimized theoretical structures are shown in Table 1. The structure of **2** with the atom numbering scheme used for Table 1 is represented in Fig. 1.

The bond length of the C1–C4 bond, at 1.361(11) Å, is similar to the bonds in other thiophene derivatives, which are typically around 1.36–1.38 Å [23–25]. The C2–C3 and C3–Br11 bonds, at 1.283(7) and 1.824(8)Å, respectively, are significantly shorter than similar bonds in other thiophene derivatives (typically 1.35–1.37 Å [23–25] and 1.86–1.90 [26–28]).These differences may be due to the nature of the packing in the crystal structure. Both calculation methods also underestimated the length of the C3–C4 bond and consistently overestimated the lengths of the C-H bonds. However, the C2–C7 bond length, experimentally observed as 1.470(9) Å, was similar to the calculated value (1.496 (B3LYP) or 1.501 (HF)) and to the experimental values for similar bonds in related compounds (1.505 [29] and 1.490 Å [30]). So, there was good agreement between the experimental and calculated values of the bonds. The linear regression correlation coefficients (R^2) were reasonable (0.951 for B3LYP and 0.945 for HF).

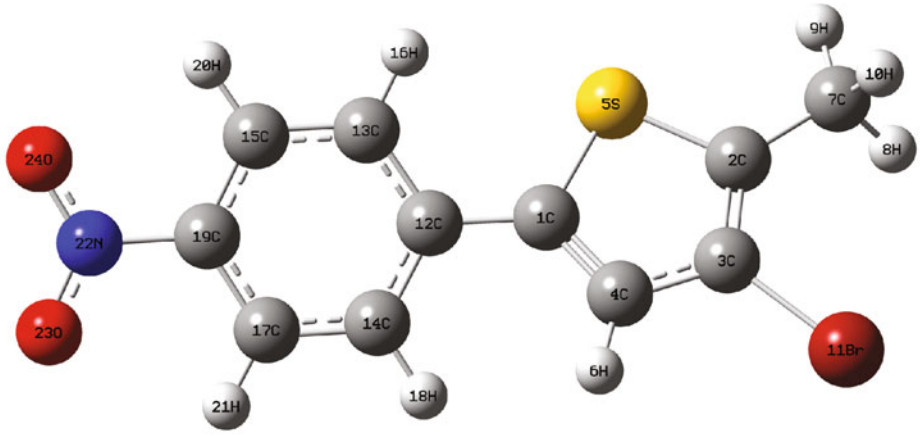

Fig. 1. The numbering of atoms of the molecule of **2**.

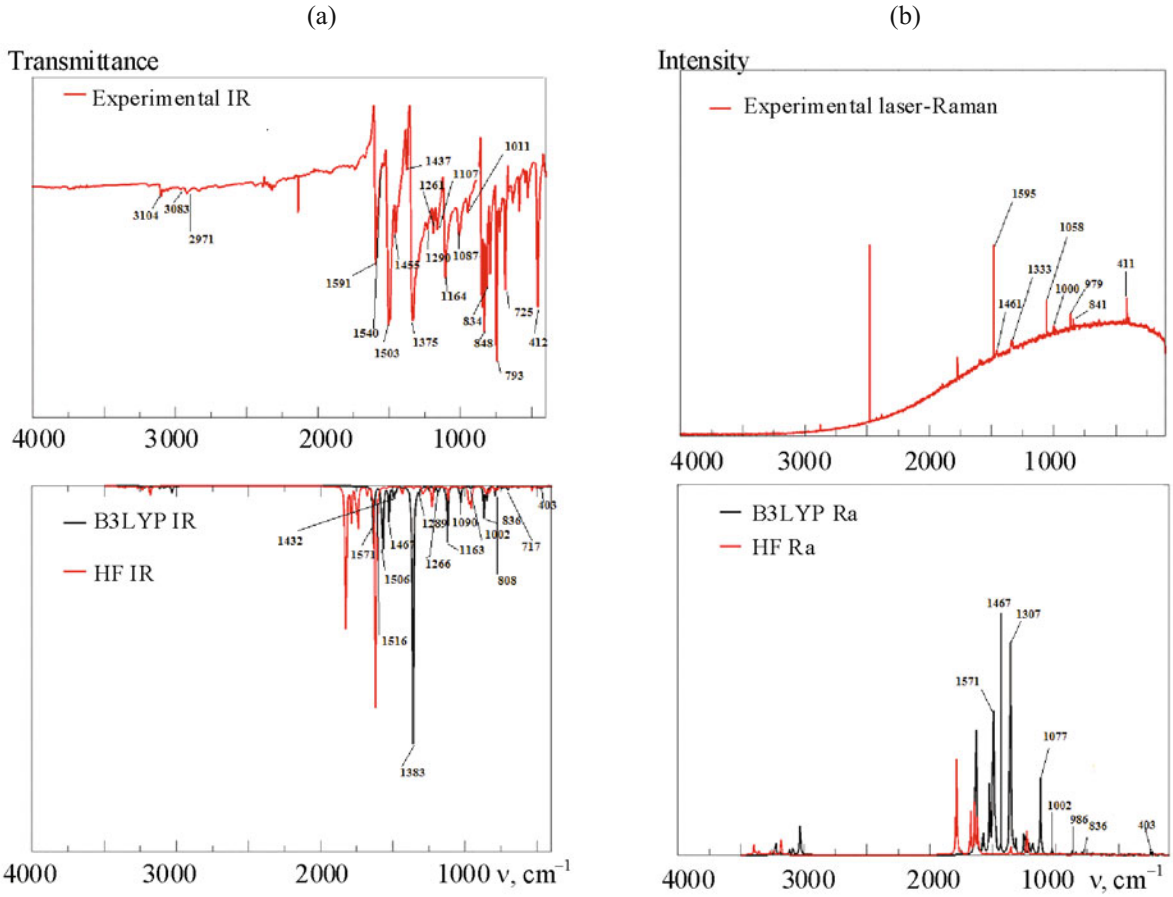

Fig 2. Comparison of observed and calculated infrared (a) and Raman (b) spectra of **2**.

The linear regression correlation coefficients (R^2) were less (0.848 for B3LYP and 0.876 for HF) for the calculated bond angles in compound **2**. Many of the calculated bond angles showed a reasonable correlation with the observed angles, but the largest variations ((9.6/9.0 for B3LYP/HF (S5–C2–C7), 7.5/7.1 (C3–C2–S5), 6.7/5.3 (C2–C3–Br11), 5.4/5.1 (C1–C4–C3), 5.7/4.8 (C4–C3–Br11) and 3.1/3.2^o (C3–C4–H6)) were for the angles of the bonds inside the thiophene ring and around it, which resulted in decreasing the linear regression coefficients.

TABLE 1. Experimental and Calculated Geometric Parameters for Compound **2**

Geometric parameters	Experimental	Calculated	
		B3LYP/6-311++G(d,p)	HF/6-311++G(d,p)
Bond lengths, Å			
C1–C4	1.361(11)	1.373	1.347
C1–S5	1.735(8)	1.753	1.738
C1–C12	1.466(13)	1.463	1.477
C2–C3	1.283(7)	1.369	1.344
C2–S5	1.736(8)	1.742	1.734
C2–C7	1.470(9)	1.496	1.501
C3–C4	1.501(11)	1.420	1.433
C3–Br11	1.824(8)	1.906	1.891
C4–H6	0.950	1.081	1.072
C7–H8	0.980	1.093	1.082
C7–H9	0.980	1.091	1.084
C7–H10	0.980	1.095	1.086
C12–C13	1.404(14)	1.407	1.393
C12–C14	1.390(14)	1.408	1.394
C13–C15	1.390(15)	1.387	1.381
C13–H16	0.950	1.084	1.074
C14–C17	1.381(15)	1.386	1.380
Bond lengths, Å			
C14–H18	0.950	1.083	1.074
C15–C19	1.371(16)	1.391	1.381
C15–H20	0.950	1.081	1.072
C17–C19	1.376(16)	1.392	1.382
C17–H21	0.950	1.081	1.072
C19–N22	1.491(13)	1.473	1.464
N22–O23	1.235(13)	1.226	1.188
N22–O24	1.209(12)	1.226	1.188
R^2		0.9507	0.9454
Bond angles, degrees			
C4–C1–S5	111.1(8)	110.0	110.5
C4–C1–C12	130.6(9)	128.4	127.6
S5–C1–C12	118.3(6)	121.7	121.8
C3–C2–S5	117.0(6)	109.1	109.5
C3–C2–C7	135.1(10)	129.5	129.9
S5–C2–C7	107.8(9)	121.3	120.6
C2–C3–C4	108.9(8)	115.2	114.8
C2–C3–Br11	129.3(6)	122.8	124.2

TABLE 1. (Continued)

Geometric parameters	Experimental	Calculated	
		B3LYP/6-311++G(d,p)	HF/6-311++G(d,p)
Bond angles, degrees			
C4–C3–Br11	108.9(8)	122.0	121.1
C1–C4–C3	113.1(11)	112.8	112.5
C1–C4–H6	123.4	124.1	124.4
C3–C4–H6	123.4	123.2	123.1
C1–S5–C2	89.9(4)	92.9	92.7
C2–C7–H8	109.5	110.5	110.4
C2–C7–H9	109.5	111.5	110.9
C2–C7–H10	109.5	110.9	110.6
H8–C7–H9	109.5	108.3	108.5
H8–C7–H10	109.5	107.5	108.3
H9–C7–H10	109.5	108.0	108.2
C1–C12–C13	120.7(9)	121.4	121.0
C1–C12–C14	121.2(9)	120.3	120.0
C13–C12–C14	118.0(9)	118.3	119.0
C12–C13–C15	120.2(10)	121.2	120.8
C12–C13–H16	119.9	119.9	120.1
C15–C13–H16	119.9	119.0	119.1
C12–C14–C17	122.1(10)	121.1	120.8
C12–C14–H18	119.0	119.8	119.9
C17–C14–H18	119.0	119.1	119.3
C13–C15–C19	118.7(11)	118.9	118.8
C13–C15–H20	120.6	121.4	121.1
C19–C15–H20	120.6	119.6	120.1
C14–C17–C19	117.9(10)	119.0	118.8
C14–C17–H21	121.1	121.4	121.1
C19–C17–H21	121.1	119.6	120.1
C15–C19–C17	123.1(1)	121.5	121.9
C15–C19–N22	119.0(10)	119.2	119.1
C17–C19–N22	117.9(10)	119.2	119.1
C19–N22–O23	118.3(10)	117.7	117.6
C19–N22–O24	118.1(10)	117.7	117.6
O23–N22–O24	123.6(9)	124.6	124.8
R^2		0.8482	0.8758

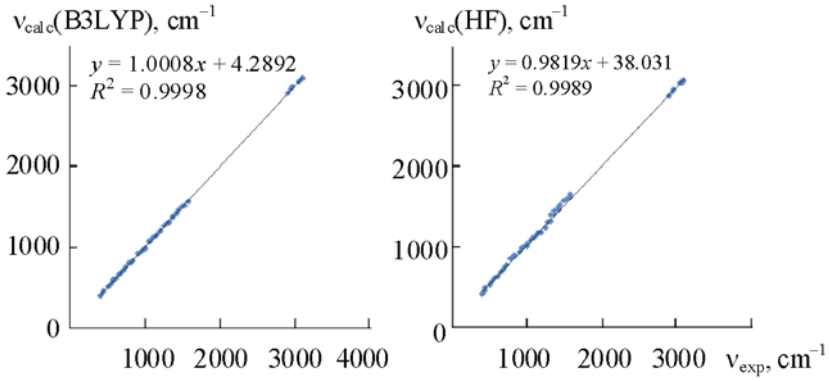

Fig. 3. Correlation graphics of experimental and theoretical (scaled) wave numbers of **2**.

Vibrational analysis. The experimental FT-IR (Fig. 2a) and Raman spectra (Fig. 2b) for compound **2** were compared with the calculated spectra (see Table 2, where the calculated harmonic vibrational frequencies scaled according to published recommendations (B3LYP and HF) [18, 19], observed frequencies, and detailed potential energy distribution (PED) are represented). The calculated modes, within each fundamental wave number, are numbered downwards from the largest to the smallest frequency. The experimental frequencies for compound **2** were obtained for the solid phase, but the calculated harmonic ones relate to the gas phase.

The reasonable agreement between the wave numbers calculated by the B3LYP method and the observed values (Fig. 3, Table 2) indicates a reasonable correlation. Indeed, the linear relationship between the calculated (B3LYP) and experimental wave numbers is given by the equation for the B3LP method

$$\nu_{cal} = 1.0008\nu_{exp} - 4.2892 , \quad (1)$$

for which R^2 = 0.9998. It indicates that the calculated and experimental values differ by 4 cm^{-1}. By contrast, there was substantial disagreement (over 70 cm^{-1} in the worst cases) between the calculated frequencies and the observed ones for the case of the HF calculations. Nevertheless, the calculated and experimental values showed a reasonably good linear relationship to each other (Fig. 3), as represented by the equation for the HF method

$$\nu_{cal} = 0.9819\nu_{exp} + 38.031 , \quad (2)$$

for which R^2 = 0.9989. Clearly, if the scaling factor used for converting the HF calculated frequencies is 0.9218 (i.e., 0.9051/0.9819) instead of the recommended 0.9051, then the value is reduced by 38 cm^{-1}, and one can ob-serve much closer agreement between the observed and calculated wave numbers, even using the HF method.

Bromo-methylthiophene group vibrations. In five heterocycles, e.g., furan, pyrrole, and thiophene, the stretching vibration frequencies of the C–H bonds are expected at 3100–3000 cm^{-1}, with multiple weak bands, but the frequency of the C–H bond vibration is highly affected by the substituent type [31, 32]. In the C–H plane, the bond vibrations are less sensitive to the substituent type and appear at 1100–1500 cm^{-1} [21]. Out of the C–H plane, the vibrations of the bonds occur at 800–1000 cm^{-1} [32]. For compound **2**, the only thiophene C–H stretching vibration was observed at 3104 cm^{-1} (FT-IR) and calculated as 3097 (B3LYP) and 3057 cm^{-1} (HF). Athiophene C–H stretching mode was observed at 3084 cm^{-1} (FT-IR) and calculated as 3093 cm^{-1} (B3LYP) and 3063 cm^{-1} (M06-2X) for (E)-3-(4-bromo-5-methylthiophen-2-yl)acrylonitrile [15]. For thiophene-2-carbohydrazide, C–H modes resonate at 3011 cm^{-1}, 3062 cm^{-1}, and 3072 cm^{-1} as medium bands in the FT-IR spectrum and as a very weak band (3068 cm^{-1}) in the FT-Raman spectrum [33]. In the C–H plane, the bond vibrations for compound **2** were observed at 1149 cm^{-1} (FT-IR) and calculated as 1140 (B3LYP) and 1157 cm^{-1} (HF). For (E)-3-(4-bromo-5-methylthiophen-2-yl)acrylonitrile [15] in the C–H plane, the bond vibrations were observed at 1160 and 1142 cm^{-1}. Such modes calculated by different methods were: 1192 (B3LYP), 1192 (M06-2X), 1132 (B3LYP), and 1138 cm^{-1} (M06-2X) [15]. Clearly, the calculated C–H bond bands are reasonably correlated with the data from the FT-IR spectrum. For thiophene-2-carbohydrazide, in the C–H plane, the bond vibrations were observed at 1097 cm^{-1}, a weak band at 1168 cm^{-1}, and a very strong one at 1247 cm^{-1} in the FT-IR spectrum [33]. For compound **2**, out of the plane, bond modes were observed at 848/841 (FT-IR/FT-Raman) and 814 cm^{-1} (FT-IR). These modes were calculated as 836 (B3LYP)/887 (HF) and 815 (B3LYP)/864 cm^{-1} (HF), respectively. For thiophene-2-carbohydrazide [33], these bands were observed at

TABLE 2. Observed and Calculated Vibrational Frequencies for Compound **2** with 6-311++G(d,p)

No.	Assignment (PED%)	Observed frequencies, cm^{-1}		Calculated frequencies, cm^{-1} (IR intensities/Raman activity)	
		FT-IR	Raman	B3LYP	HF
ν_1	υCH (88)	3104		3099 (1.57/159.31)	3073 (1.80/73.50)
ν_2	υCH (85)	3104		3098 (1.57/48.13)	3072 (1.70/87.22)
ν_3	υCH (85)	3104		3097 (2.86/23.32)	3057 (3.42/42.74)
ν_4	υCH (93)	3083		3071 (3.12/27.64)	3038 (3.37/30.56)
ν_5	υCH (88)	3056		3061 (3.52/34.44)	3035 (3.29/34.70)
ν_6	υCH (99)	2971		2994 (6.97/80.03)	2960 (8.88/58.75)
ν_7	υCH (90)	2955		2965 (7.48/115.88)	2931 (14.40/81.91)
ν_8	υCH (91)	2912		2912 (18.88/477.45)	2877 (26.08/252.83)
ν_9	υCC (58) + υON (10)	1591	1595	1571 (116.57/1056.98)	1652 (448.38/5.38)
ν_{10}	υCC (61) + υON (10)	1591	1595	1570 (92.49/797.85)	1618 (81.97/961.55)
ν_{11}	υCC (52)	1540		1516 (61.91/215.54)	1585 (80.57/39.88)
ν_{12}	υON (58) + υCC (11)	1503		1506 (151.99/31.96)	1574 (99.32/9.52)
ν_{13}	δHCC (36)	1455	1461	1467 (83.13/640.26)	1517 (19.41/418.10)
ν_{14}	δHCH (56)	1437		1437 (22.37/2185.03)	1487 (8.16/530.49)
ν_{15}	δHCH (64) + τHCCC (18)	1437		1432 (13.90/44.50)	1466 (545.95/360.38)
ν_{16}	δHCH (72) + τHCCC (18)	1437		1420 (11.96/235.41)	1454 (9.43/7.53)
ν_{17}	υCC (35) + δHCC (11)	1375		1383 (1.29/128.00)	1448 (7.60/34.68)
ν_{18}	δHCH (90)	1375		1364 (0.25/13.84)	1401 (2.75/17.58)
ν_{19}	υON (26) + υCC (13)	1329	1333	1310 (161.04/602.57)	1394 (3.13/3.56)
ν_{20}	υON (51)	1329	1333	1307 (598.26/1837.27)	1310 (7.41/5.73)
ν_{21}	δHCC (43) + υCC (22)	1290		1289 (16.97/41.78)	1297 (30.28/12.15)
ν_{22}	δHCC (30) + υCC (17)	1261		1266 (17.81/132.02)	1229 (8.06/86.53)
ν_{23}	υCC (39) + δCCC (14)	1209		1202 (11.31/295.54)	1175 (7.35/17.53)
ν_{24}	δHCC (59) + υCC (37)	1164		1163 (14.26/98.77)	1167 (24.35/16.35)
ν_{25}	δHCC (45)	1149		1140 (20.54/136.38)	1157 (12.97/11.43)
ν_{26}	υCC (31) + τHCCC (20)	1107	1104	1127 (3.98/40.83)	1117 (7.34/52.86)
ν_{27}	δHCC (56) + υCC (14)	1087		1090 (10.63/2.67)	1112 (48.83/203.69)
ν_{28}	υNC (21) + υCC (20) + δHCC (10)	1059	1058	1077 (133.06/666.77)	1076 (0.23/2.23)
ν_{29}	τHCCC (74) + δHCH (16)	1011	1000	1002 (8.90/4.43)	1036 (6.30/0.17)
ν_{30}	δCCC (34) + τHCCC (12)	1011		991 (25.01/25.39)	1011 (32.68/12.02)
ν_{31}	δCCC (20) + τHCCC (17)	1011	979	986 (24.00/41.84)	1007 (0.46/0.09)
ν_{32}	τHCCC (70)	965		958 (0.08/0.51)	1000 (0.43/9.16)
ν_{33}	τHCCC (70)	950		949 (1.48/0.68)	990 (0.97/1.06)
ν_{34}	δCCC (38)	917		924 (7.83/13.87)	934 (8.55/18.49)
ν_{35}	δONO (18) + τHCCC (11)	848	841	836 (33.03/21.37)	887 (5.28/6.09)

TABLE 2. (Continued)

No.	Assignment (PED%)	Observed frequencies, cm^{-1}		Calculated frequencies, cm^{-1} (IR intensities/Raman activity)	
		FT-IR	Raman	B3LYP	HF
ν_{36}	δONO (32)	834	841	834 (44.91/13.32)	877 (66.20/18.35)
ν_{37}	τHCCC (47)	814		815 (32.73/2.48)	864 (56.58/2.12)
ν_{38}	τHCCC (58)	793		808 (6.18/22.77)	850 (0.23/6.64)
ν_{39}	υSC (29) + υBrC (15)	747		759 (26.16/23.66)	774 (33.96/7.14)
ν_{40}	γOCON (33) + γNCCC (13) + τCCCC (10)	725		717 (7.69/6.06)	753 (26.81/5.85)
ν_{41}	δCCC (15) + δONO (13) + υCC (11)	706		703 (5.58/10.71)	718 (14.16/10.16)
ν_{42}	γOCON(21) + υSC(19)	685		677 (10.45/15.10)	701 (11.95/1.07)
ν_{43}	γOCON (21) + υSC (13) + τCCCC (12)	663		671 (5.24/10.32)	678 (1.15/8.70)
ν_{44}	δCCC (55) + υCC (14)	623		619 (0.86/6.92)	624 (0.17/6.76)
ν_{45}	δSCC (29) + υCC (14) + δCCC (11)	586		606 (6.03/6.51)	612 (3.31/4.38)
ν_{46}	τCCCC (37) + γBrCCC (17) + τSCCC (10)	575		575 (2.78/3.89)	601 (2.86/2.96)
ν_{47}	τSCCC (22) + γCCCC (13)	545		532 (0.77/1.32)	558 (1.64/1.40)
ν_{48}	δONC (55) + δNCC (13)	523		514 (1.41/3.05)	523 (3.05/1.80)
ν_{49}	γCCCC (28) + γNCCC (11)	456		461 (10.50/1.92)	483 (12.09/0.59)
ν_{50}	υNC (32) + δCCC (19) + δONO (10)	456		442 (6.14/0.28)	450 (10.70/0.33)
ν_{51}	τCCCC (29)	412	411	403 (0.37/5.60)	414 (0.01/2.83)
ν_{52}	τCCCC (12) + δCCS (10)	412	411	401 (0.94/4.82)	400 (0.90/0.88)
ν_{53}	δCCS (23) + υBrC (20)			339 (0.72/5.53)	352 (1.51/2.31)
ν_{54}	τCCCC (16) + γCCSC (15) + υBrC (13)			319 (1.13/6.48)	335 (0.58/7.27)
ν_{55}	υBrC (11) + δNCC (11)			286 (0.49/0.63)	289 (0.77/0.20)
ν_{56}	γCCSC (20) + τBrCCC (11) + δNCC (10)		250	237 (0.16/0.54)	252 (0.38/0.57)
ν_{57}	υCC(14) +υBrC(12)+δNCC(11)+δCCC(10)		208	208 (0.11/1.98)	213 (0.39/3.37)
ν_{58}	δCCS (22) + δNCC (18) + δCCC (11)		208	201 (3.16/1.73)	203 (3.54/1.75)
ν_{59}	δBrCC (36)		159	159 (0.42/3.72)	166 (0.73/2.54)
ν_{60}	τSCCC (40) + τBrCCC (34)			152 (0.97/5.15)	155 (1.19/2.21)
ν_{61}	δCCC (27) + γNCCC (15)			120 (3.34/0.27)	125 (3.81/0.48)
ν_{62}	δCCC (46) + δBrCC (10)			62 (0.76/1.23)	61 (0.57/1.06)
ν_{63}	τONCC (74) + τSCCC (10)			56 (0.26/3.32)	51 (0.17/1.64)
ν_{64}	τHCCC (51) + τCCCC (13) + τONCC (10)			48 (0.49/1.33)	42 (1.01/0.58)
ν_{65}	τCCCC (34) + γCCCC (22)			40 (0.55/0.95)	28 (0.19/5.22)
ν_{66}	τCCCC (77) + τONCC (14)			27 (0.35/6.28)	20 (0.07/1.23)

Note. υ, stretching; δ, in-plane bending; γ, out-of-plane bending; τ, torsion; PED, potential energy distribution. Values of the potential energy distribution (PED) presented after experimental frequencies were calculated by B3LYP/6-311++G(d,p) method; values less than 10% are not shown.

837 (FT-IR) and 845 cm^{-1} (FT-Raman). For (*E*)-3-(4-bromo-5-methylthiophen-2-yl)acrylonitrile [15], out of the plane, modes were observed at 834 and 794 cm^{-1} and calculated as 828 cm^{-1} (B3LYP)/834 cm^{-1} (M06-2X) and 799 cm^{-1} (B3LYP)/803 cm^{-1} (M06-2X), respectively [15].

The C=C stretching vibrations within the thiophene rings are of aromatic character [34]. For compound **2**, the C=C stretching vibrations showed two modes, observed at 1540 and 1503 cm^{-1} (FT-IR) and calculated as 1516 (B3LYP)/1585 (HF) and 1506 (B3LYP)/1574 cm^{-1}, respectively. From the PED analysis, we conclude that the contributions of the C=C stretching vibrations for the two modes are 52% (1540 cm^{-1}) and 11% (1503 cm^{-1}), respectively. The main 58% contribution for the mode 1503 cm^{-1} is from the O=N stretching vibrations. For 3-ethynylthiophene, the C=C stretching vibration was observed at 1516 cm^{-1} and two modes were calculated at 1525 and 1413 cm^{-1} [25]. For (*E*)-3-(4-bromo-5-methylthiophen-2-yl)acrylonitrile [15] the bands that resonated at 1600, 1517, and 1460 cm^{-1} were observed in the FT-IR spectrum. For compound **2,** other C–C modes in the thiophene ring were observed at 1329/1333 (FT-IR/FT-Raman), 1290 (FT-IR) and 1261 cm^{-1} (FT-IR). They were calculated as 1310 (B3LYP)/1394 (HF), 1289 (B3LYP)/1297 (HF) and 1266 (B3LYP)/1229 cm^{-1} (HF) and assigned by PED. For 3-ethynylthiophene [25] the C–C mode was calculated at 1355 cm^{-1} and observed at 1358 (FT-IR) and 1357 cm^{-1} (FT-Raman).

C–S bond vibrations cannot always be distinguished in thiophene ring systems [35], although for thiophene itself C–S modes appear at 872/753 and 870/750 cm^{-1} for the vapor and liquid phases, respectively [36]. For compound **2**, three mixed mode bands (according to the PED analysis), incorporating contributions from the C–S mode, were seen at 747, 685, and 663 cm^{-1} (FT-IR) and calculated at 759 (B3LYP)/774 (HF), 677 (B3LYP)/701 (HF) and 671 (B3LYP)/678 cm^{-1} (HF), respectively. Karabacak et al. [37] calculated three C–S modes at 848, 846, and 641 cm^{-1} for (*S*)-*N*-benzyl-1-phenyl-5-(thiophen-3-yl)-4-pentyn-2-amine. For (*E*)-3-(4-bromo-5-methylthiophen-2-yl)acrylonitrile [15], the C–S stretching modes were seen at 741 and 715 cm^{-1} (FT-IR) and calculated as 777 (B3LYP)/787 (M06-2X) and 688 (B3LYP)/694 cm^{-1} (M06-2X), respectively.

For compound **2**, C–Br stretching modes were observed at 747 cm^{-1} (FT-IR) and calculated as 759 (B3LYP)/774 (HF), 319 (B3LYP)/335 (HF) and 286 (B3LYP)/289 cm^{-1} (HF) as three modes. One in-plane Br1–C2–C3 (δBrCC) bending mode was observed at 159 cm^{-1} (FT-Raman) and calculated at 159/166 and 62/61 cm^{-1} by the B3LYP/HF methods. One out-of-plane τBrCCC bending mode was observed at 250 cm^{-1} (FT-Raman), but two were calculated, at 237/252 and 152/155 cm^{-1} by the B3LYP/HF methods.

CH_3 stretching vibrations generally appear at 2950–3050 (asymmetric) and 2900–2950 cm^{-1} (symmetric) [38, 39]. For compound **2**, CH_3 asymmetric stretching modes were calculated as 2994 (B3LYP)/2960 (HF) and 2965 (B3LYP)/2960 cm^{-1} (HF) and were observed at 2971 and 2955 cm^{-1} in the FT-IR spectrum, while one CH_3 symmetric mode was calculated as 2912 (B3LYP)/2877 cm^{-1} (HF) and was observed at 2912 cm^{-1} (FT-IR). CH_3 symmetrical bending deformations ($\delta_s CH_3$) are typically at 1400–1485 cm^{-1} [38] and for compound **2** were calculated as 1437 (B3LYP)/1487 (HF) and 1420 (B3LYP)/1454 cm^{-1} (HF). They were seen as a single envelope at 1437 cm^{-1} in the FT-IR spectrum. For various methyl-containing thiophene derivatives, symmetric deformations ($\delta_s CH_3$) appear at 1380 ± 25 cm^{-1} [38]. For compound **2**, this band was observed at 1375 cm^{-1} (FT-IR) and calculated as 1364 (B3LYP)/1401 cm^{-1} (HF). Aromatic compounds carrying a methyl group display a methyl rocking mode (ρCH_3) in the neighborhood of 1045 cm^{-1} [38], while a second rocking mode at 970 ± 70 cm^{-1} region [38] is difficult to find among the C–H out-of-plane deformations. For compound **2**, ρCH_3 modes were seen at 1011 (FT-IR)/1000 (FT-Raman) and 1011 (FT-IR)/979 cm^{-1} (FT-Raman) and calculated at 1002 (B3LYP)/1036 (HF) and 986 (B3LYP)/1007 cm^{-1} (HF). The methyl twisting mode is often seen in the 1470–1440 cm^{-1} region [38]. For compound **2**, this mode was observed at 1437 cm^{-1} (FT-IR) and calculated as 1432 (B3LYP)/1466 cm^{-1} (HF).

Nitrophenyl group vibrations. C–H stretching vibrations generally resonate at 3100–3000 cm^{-1}, and this region is used for identification of such vibrations [40, 41]. For compound **2**, C–H stretching modes were seen at 3104, 3083, and 3056 cm^{-1} in the FT-IR spectrum, but were not seen in the Raman spectrum. Five C–H stretching modes were calculated at 3099 (B3LYP)/3073 (HF), 3098 (B3LYP)/3072 (HF), 3097 (B3LYP)/3057 (HF), 3071 (B3LYP)/3038 (HF), and 3061 (B3LYP)/3035 cm^{-1} (HF). In-plane aromatic C–H bending vibrations typically appear at 1300–1000 cm^{-1} [40]. For compound **2**, in-plane C–H bending modes were seen at 1375 (FT-IR), 1261 (FT-IR), 1164 (FT-IR), 1087 (FT-IR), and 1059 (FT-IR)/1058 cm^{-1} (Raman). The calculated in-plane bending modes were 1383 (B3LYP)/1448 (HF), 1266 (B3LYP)/1229 (HF), 1163 (B3LYP)/1167 (HF), 1090 (B3LYP)/1112 (HF), and 1077 (B3LYP)/1076 cm^{-1} (HF). C–H out-of-plane bending modes are seen at 700–1000 cm^{-1} [38–41]. For compound **2**, C–H out-of-plane bending modes were observed at 965 (FT-IR), 950 (FT-IR), 848 (FT-IR)/841 (Raman), 814 (FT-IR), and 793 cm^{-1} (FT-IR). They were calculated as 958 (B3LYP)/1000 (HF), 949 (B3LYP)/990 (HF), 836 (B3LYP)/887 (HF), 815 (B3LYP)/864 (HF), and 808 (B3LYP)/850 cm^{-1} (HF).

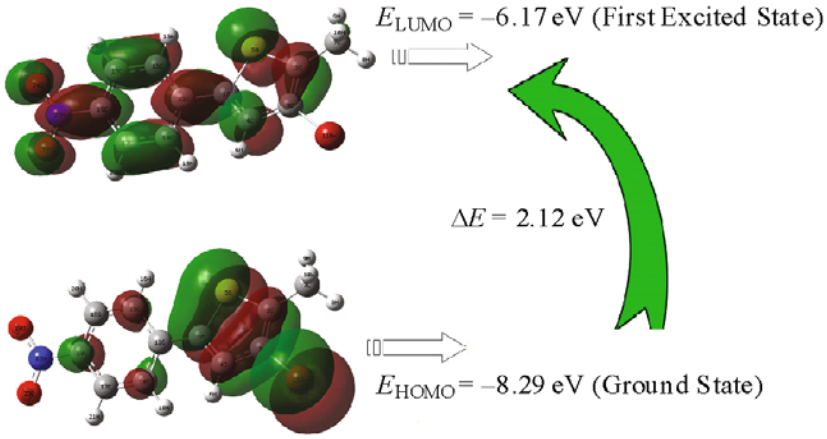

Fig. 4. Calculated HOMO–LUMO plots of **2**.

TABLE 3. HOMO–LUMO Energy Gaps and Related Molecular Properties for Compound **2**

Molecular properties	B3LYP/6-311++G(d,p)	HF/6-311++G(d,p)
Energies (a.u.)	–3601.45	–3595.13
E_{HOMO} (eV)	–8.29	–8.30
E_{LUMO} (eV)	–6.17	–6.09
Energy Gap (eV)	2.12	2.21
Ionization potential (I)	8.29	8.30
Electron affinity (A)	6.17	6.09
Global Hardness (η)	1.06	1.11
Chemical Potential (μ)	–7.23	-7.20
Electrophilicity (ψ)	24.66	23.35
Softness (ζ)	0.47	0.45
Dipole moment (debye)	5.54	5.01

Note. $I = -E_{HOMO}$; $A = -E_{LUMO}$; $\eta = 1/2(E_{LUMO} - E_{HOMO})$; $\mu = 1/2(E_{LUMO} + E_{HOMO})$; $\psi = \mu^2/2\eta$; $\zeta = 1/2\eta$.

Aromatic ring C–C stretching modes normally appear at 1590–1430 cm^{-1} [42–44]. For compound **2**, C–C stretching modes were observed at 1591 (FT-IR)/1595 (Raman), 1503 (FT-IR), 1375 (FT-IR), 1329 (FT-IR)/ 1333 (Raman), 1290 (FT-IR) and 1261 cm^{-1} (FT-IR). Clearly, the last four bands are outside the normal range, but the calculations revealed all of the bands, at 1571 (B3LYP)/1652 (HF), 1570 (B3LYP)/1618 (HF), 1506 (B3LYP)/1574 (HF), 1383 (B3LYP)/1448 (HF), 1310 (B3LYP)/1394 (HF), 1289 (B3LYP)/1297 (HF), and 1266 (B3LYP)/1229 cm^{-1} (HF). CCC in-plane bending modes typically appear at 640–800 cm^{-1}, while out-of-plane bending modes appear at 475–580 cm^{-1} [44, 45]. For compound **2**, in-plane CCC modes were observed at 706 (FT-IR), 623 (FT-IR), and 586 cm^{-1} (FT-IR) and calculated as 703 (B3LYP)/718 (HF), 619 (B3LYP)/624 (HF), and 606 (B3LYP)/612 cm^{-1} (HF). CCC out-of-plane modes were observed at 545 (FT-IR), 456 (FT-IR), and 412 (FT-IR)/411 (Raman) and calculated at 532 (B3LYP)/558 (HF), 461 (B3LYP)/483 (HF), 403 (B3LYP)/414 (HF), and 401 (B3LYP)/400 cm^{-1} (HF).

Aromatic nitro compounds show strong absorption bands at 1570–1485 cm^{-1} (asymmetric stretching) and 1370–1320 cm^{-1} (symmetric stretching) [46]. For compound **2**, asymmetric NO_2 modes were observed at 1591 (FT-IR)/1595 (Raman) and 1503 cm^{-1} (FT-IR) and calculated at 1571 (B3LYP)/1652 (HF), 1570 (B3LYP)/1618 (HF), and 1506 (B3LYP)/1574 cm^{-1} (HF). Symmetric stretching modes were observed as a single band at 1329 (FT-IR)/1333 cm^{-1} (Raman) and calculated at 1310 (B3LYP)/1394 (HF) and 1307 (B3LYP)/1310 cm^{-1} (HF). NO_2 group deformation vibrations

appear within the low frequency region [47, 48]. For example, a strong band at 818 cm^{-1} in 5-bromo-2-nitropyridine was assigned to a NO_2 scissoring mode [49]. For compound **2**, NO_2 scissoring vibrations were observed at 848 (FT-IR)/841 cm^{-1} (Raman) and calculated at 836 (B3LYP)/887 (HF) and 834 (B3LYP)/877 cm^{-1} (HF). The remainder of the observed and calculated wave numbers and assignments of the present molecule are shown in Table 2.

HOMO–LUMO analysis. The HOMO–LUMO orbitals affect the chemical stability of organic compounds [50]. Reactive (soft) molecules have a low HOMO–LUMO energy gap [51], and the kinetic stability and reactivity of molecules can be better understood through the frontier molecular orbital energy gap [52–54]. The LUMO and HOMO energies for compound **2** were calculated by the B3LYP/6-311++G(d,p) and HF/6-311++G(d,p) methods and are represented in Fig. 4. The HOMO of **2** is located on the thiophene ring, C13, C19, C14 and over the Br atom. The LUMO is more focused on the thiophene ring and over the nitrophenyl group. The HOMO–LUMO energy gap for compound **2** and the related molecular parameters [55, 56] are shown in Table 3. The ionization potential for compound **2** is 8.29 (B3LYP) or 8.30 eV (HF).

Conclusions. The vibrational spectrum of 3-bromo-2-methyl-5-(4-nitrophenyl)thiophene (**2**) was studied experimentally (FT-IR and Raman spectra) and theoretically (DFT/B3LYP and HF methods). The theoretical optimized geometric parameters, bond lengths and angles, as well as vibrational frequencies, were found to be in quite good agreement with the corresponding experimental data and with the values reported for similar compounds. The charge transfer within compound **2** was understood with the help of the data obtained from calculation of the HOMO and LUMO orbitals and their energies. The present study provides significant information for the possible application of **2** in pharmacological investigations.

Acknowledgments. The authors are grateful to the Deanship of Scientific Research at King Saud University for funding through the research group project RGP-239 and EPSRC for the grant which supplied the MS instrumentation used in this study.

REFERENCES

1. M. Irie, *Chem. Rev*., **100**, 1685–1716 (2000).
2. M. Balter, S. Li, J. R. Nilsson, J. Andreasson, and U. Pischel, *J. Am. Chem. Soc*., **135**, 10230–10233 (2013).
3. J.-C. Boyer, C-J. Carling, B. D. Gates, and N. R. Branda, *J. Am. Chem. Soc*., **132**, 15766–15772 (2010).
4. T. C. Pijper, T. Kudernac, W. R. Browne, and B. L. Feringa, *J. Phys. Chem. C*, **117**, 17623–17632 (2013).
5. N. Soh, K. Yoshida, H. Nakajima, K. Nakano, T. Imato, T. Fukaminatob, and M. Irie, M. *Chem. Commun*., 5206–5208 (2007).
6. E. Negishi (Ed.), *Handbook of Organopalladium Chemistry for Organic Synthesis*, Wiley-Interscience, New York, Part III (2002), 213 p.
7. J. J. Li and G. W. Gribble, *Palladium in Heterocyclic Chemistry*; Pergamon, Amsterdam (2000).
8. J. J. Dong, D. Roy, J. R. Roy, M. Ionita, and H. Doucet, *Synthesis*, 3530–3546 (2011).
9. G. Vamvounis and D. Gendron, *Tetrahedron Lett*., **54**, 3785–3787 (2013).
10. W. Renjie, P. Shouzhi, L. Gang, and C. Bing, *Tetrahedron*, **69**, 5537–5544 (2013).
11. K. A. Browne, D. D. Deheyn, G. A. El-Hiti, K. Smith, and I. Weeks, *J. Am. Chem. Soc*., **133**, 14637–14648 (2011).
12. K. Smith, G. A. El-Hiti, and A. S. Hegazy, *Chem. Commun*., **46**, 2790–2792 (2010).
13. K. Smith, G. A. El-Hiti, and A. C. Hawes, *Synthesis*, 2047–2052 (2003).
14. K. Smith, G. A. El-Hiti, G. Pritchard, and A. Hamilton, *J. Chem. Soc., Perkin Trans. I*, 2299–2304 (1999).
15. Y. Sert, A. A. Balakit, N. Öztürk, F. Ucun, and G. A. El-Hiti, *Spectrochim. Acta A*, **131**, 502–511 (2014).
16. Y. Sert, F. Ucun, G. A. El-Hiti, K. Smith, and A. S. Hegazy, *J. Spectrosc*. (2016); http://dx.doi.org/10.1155/2016/5396439.
17. G. M. Sheldrick, *Acta Crystallogr*., **A64**, 112–122 (2008).
18. A. Frish, A. B. Nielsen, and A. J. Holder, *Gauss View User Manual*, Gaussian Inc., Pittsburg, PA (2001).
19. D. C. Young, *Computational Chemistry A Practical Guide for Applying Techniques to Real-World Problems (Electronics)*, John Wiley and Sons, New York (2001).
20. *Gaussian 09, Revision A.1*, Gaussian, Wallingford CT (2009).
21. M. H. Jamróz, *Vibrational Energy Distribution Analysis VEDA 4*, Warsaw (2004).
22. M. H. Jamróz, *Spectrochim. Acta A*, **114**, 220–230 (2013).
23. G. A. El-Hiti, K. Smith, A. A. Balakit, A. Masmali, and B. M. Kariuki, *Acta Crystallogr*., **E69**, o1385 (2013).
24. A. Ünal and B. Eren, *Spectrochim. Acta A*, **114**, 129–136 (2013).
25. M. Karabacak, S. Bilgili, T. Mavis, M. Eskici, and A. Atac, *Spectrochim. Acta A*, **115**, 709–718 (2013).

26. W. T. Harrison, C. S. C. Kumar, H. S. Yathirajan, B. V. Ashalatha, and B. Narayana, *Acta Crystallogr.*, **E66**, o2477 (2010).
27. X. Li, X. Jia, and J. Li, *Acta Crystallogr*., **E69**, o848 (2013).
28. M. M. Bader, *Acta Crystallogr*., **E65**, o2119 (2009).
29. M. Akkurt, Ş. P. Yalçın, A. M. Asiri, and O. Büyükgüngör, *Acta Crystallogr*., **E64**, o923 (2008).
30. Z. H. Choban, M. Hanif, and M. N. Tahir, *Acta Crystallogr*., **E65**, o117 (2009).
31. G. Varsayani, *Assignments for Vibrational Spectra of Seven Hundred Benzene Derivatives*, vols. 1 and 2, Academic Kiado, Budapest (1973).
32. M. Jag, *Organic Spectroscopy-Principles and Applications*, 2nd ed., Narosa Publishing House, New Delhi (2001).
33. V. Balachandran, A. Janaki, and A. Nataraj, *Spectrochim. Acta A*, **118**, 321–330 (2014).
34. J. Svoboda, J. Sedlacek, J. Zednik, G. Dvorakova, O. Trhlikova, D. Redrova, H. Balcar, and J. Vohlidal, *J. Pol. Sci*., **46**, 2776–2787 (2008).
35. C. I. Sainz-Diaz, M. Francisco-Marquez, and A. Vivier-Bunge, *Theor. Chem. Acc*., **125**, 83–95 (2010).
36. T. D. Klots, R. D. Chirico, and W. V. Steele, *Spectrochim. Acta A*, **5**, 765–795 (1994).
37. M. Karabacak, C. Karaca, A. Atac, M. Eskici, A. Karanfil, and E. Köse, *Spectrochim. Acta A*, **97**, 556–567 (2012).
38. N. P. G. Roeges, *A Guide to the Complete Interpretation of Infrared Spectra of Organic Structures*, Wiley, New York (1994).
39. N. B. Colthup, L. H. Daly, and S. E. Wiberly, *Introduction to Infrared and Raman Spectroscopy*, 3rd ed., Academic Press, Boston (1990).
40. B. Smith, *Infrared Spectral Interpretation. A Systematic Approach*, CRP Press, Washington, DC (1999).
41. A. Kumar, V. Deval, P. Tandom, A. Gupta, and E. D. D'silva, *Spectrochim. Acta A*, **130**, 41–53 (2014).
42. S. Periandy and S. Mohan, *Proc. Natl. Acad. Sci. India*, **68**(A), III (1998).
43. V. R. Dani, *Organic Spectroscopy*, Tata-McGraw Hill Publishing Company, New Delhi, p. 139 (1995).
44. E. Fereyduni, M. K. Rofouei, M. Kamae, S. Ramalingam, and S. M. Sharifkhani, *Spectrochim. Acta A*, **90**, 193–201 (2012).
45. H. Abdel-Shafy, H. Perlmutter, and H. Kimmel, *J. Mol. Struct*., **42**, 37–49 (1977).
46. V. K. Kumar and V. Balachandran, *Spectrochim. Acta A*, **61**, 1811–1819 (2005).
47. A. Kovacs, G. Keresztury, and V. Izvekov, *Chem. Phys*., **253**, 193–204 (2000).
48. K. Sarojini, H. Krishnan, C. C. Kanakam, and S. Muthu, *Spectrochim. Acta A*, **108**, 159–170 (2013).
49. N. Sundaraganesan, S. Ilakiamani, H. Saleem, and S. Mohan, *Indian J. Pure Appl. Phys*., **42**, 585–590 (2004).
50. S. Ayyapan, N. Sundaraganesan, M. Kurt, T. R. Sertbakan, and M. Ozduran, *J. Raman Spectrosc*., **41**, 1379–1387 (2010).
51. K. Chaitanya, *Spectrochim. Acta A*, **86**, 159–173 (2012).
52. E. Kavitha, N. Sundaraganesan, and S. Sebastian, *Indian J. Pure Appl. Phys*., **48**, 20–30 (2010).
53. A. Jayaprakash, V. Arjunan, and S. Mohan, *Spectrochim. Acta A*, **81**, 620–630 (2011).
54. S. Subashchandrabose, H. Saleem, Y. Erdogdu, G. Rajarajan, and V. Thanikachalam, *Spectrochim. Acta A*, **82**, 260–269 (2011).
55. T. Vijayakumar, I. Hubert Joe, C. P. R. Nair, and V. S. Jayakumar, *Chem. Phys*., **343**, 83–99 (2008).
56. M. Govindarajan, M. Karabacak, A. Suvitha, and S. Periandy, *Spectrochim. Acta A*, **89**,137–148 (2012).